Scale in Remote Sensing and GIS

Edited by
Dale A. Quattrochi
National Aeronautics and Space Administration
Huntsville, Alabama
and
Michael F. Goodchild
University of California
Santa Barbara, California

LEWIS PUBLISHERS
Boca Raton New York London Tokyo

Cover: Color composite image of processed Landsat Thematic Mapper image recorded September 14, 1989 over the central Amazon River approximately 50 km upstream from the town of Óbidos and 650 km downstream from the town of Manaus. The record flood of 1989 has receded approximately 2 m, the floodplain is draining, and flow is from left to right (west to east) in the main channel which is 4 to 6 km wide. The color of the main channel (red) indicates relatively high suspended-sediment concentrations in the water. The dark blue color indicates relatively clear water, and blue-green indicates tropical forest. Image processing completed by A. K. Mertes, Department of Geography, University of California, Santa Barbara. Raw image provided by R. Almeida Filho of INPE, Brazil.

Acquiring Editor:	Neil Levine
Project Editor:	Joan Moscrop
Marketing Manager:	Greg Daurelle
Direct Marketing Manager:	Arline Massey
Cover design:	Denise Craig
Manufacturing:	Sheri Schwartz

Library of Congress Cataloging-in-Publication Data

Scale in remote sensing and GIS / edited by Dale A. Quattrochi and Michael F. Goodchild
p. cm.
Includes bibliographical references and index.
ISBN 1-56670-104-X
1. Geographic information systems. 2. Remote sensing. I. Quattrochi, Dale A.
II. Goodchild, Michael F.
G70.212.S28 1996
621.36'78—dc20 96-27156
CIP

International Standard Book Number 1-56670-104-X
Library of Congress Card Number 96-27156
Printed in the United States of America 1 2 3 4 5 6 7 8 9 0
Printed on acid-free paper

CHAPTER 4

Multiresolution Covariation Among Landsat and AVHRR Vegetation Indices

Lee De Cola

INTRODUCTION

The treatment of data at multiple scales is well-established in the spatial analytical literature (Bian and Walsh, 1993; Franklin, 1994; Frank et al., 1994; Lambin et al., 1995) and is becoming increasingly common in broader discussions of biophysical and landscape processes (Meentemeyer and Box, 1987; Turner and Gardner, 1992). Quattrochi (1993) provides a "lexicon of scale" that presents the fundamental dimensions of the problem. I would rearrange his discussion by prioritizing the issues:

- Space: absolute and relative
- Measurement: resolution and extent
- Analysis: scaling and measures of spatial complexity (Stoms, 1994)
- Objects and processes: resolution element (fine level) and characteristic size (coarse level) (Cullinan and Thomas, 1992)

This organization begins with abstract space, which forms a framework for measurement that produces data to be analyzed at multiple resolutions for the characterization of processes and the identification of objects. In this chapter the first and last issues are not explored as the data are already given; the focus is more on technique than on characterization either of the landscape in general or of vegetation in particular.

The typical approach to scale issues argues that each phenomenon requires a specific scale of data for its characterization (Jensen, 1986). This book demonstrates how information from a range of scales is critical to the understanding of spatial processes. In keeping with Quattrochi's system, all data may be considered as

existing in a space of four conceptual dimensions, each with its unique characteristics:

- Space — continuous and unbounded (Getis and Franklin, 1987)
- Time — continuous and bounded in one direction (the future) (Peuquet, 1993)
- Feature — discontinuous and unbounded (Buttenfield, 1994)
- Scale — continuous and bounded in one direction (the finest available resolution) (Basseville et al., 1992)

This scheme augments the usual notion of features in space and time by highlighting the nature of scale itself as a hierarchical framework within which phenomena may be studied. Each of the first three dimensions presents us with (usually strongly related) scale issues. Moreover, time and scale have directionality. Time moves from past through present to future, and we have more confidence in historical data based on prior states of a system than in future projections. Scale moves from coarse to fine, and we become less certain of lower-level (finer) representations based on interpolations of spatial data than on higher-level generalizations. Finally, spatial scale itself is a continuum that reveals useful information about phenomena only when we look at multiple scales.

Nevertheless, the word "scale" will be avoided here because it has strict cartographic and loose physical meanings that are opposite in intent, and because the term is better constrained to references to some continuum (small to big) than applied to specific levels within the range. As this chapter is concerned with satellite data, the term "resolution" is used instead. The next sections formalize these ideas, introduce data to illustrate them, and then analyze the data. The chapter concludes with a broader view of this research.

MULTIRESOLUTION ANALYSIS

Let $l = 0,...,L$ be a resolution level, where larger values of l denote larger (coarser) physical resolutions of observation or analysis. Let a given dataset A_0 consist of measurements made at some resolution considered to be level-0 for the available data (for example, for the Landsat thematic mapper (TM) level-0 is based on 30-m instantaneous field of view (Richards, 1986)). The integer index l will correspond to the relative physical size of the units of observation, in this case grid cells. The exploration of scaling in data is sometimes based on multiple levels of observations but usually depends upon the analysis of original data at multiple resolutions created by some kind of a generalization operator $g(\ )$ that should not introduce artifacts into the data. Consider the production of $A_1 = g(A_0)$ where A_1 is some generalized version of A_0. This process can be repeatedly applied

$$g^2(A) = A_{l+2} = g(A_{l+1}) = g(g(A_l)) \tag{1}$$

to produce a recursively constructed data pyramid

$$\{A\} = \{A_l: l = 0,...,L\} \quad (2)$$

based on level-0 (Samet, 1989). There are many ways to generalize data, such as sampling, filtering, and averaging, which are appropriate for various kinds of objects and fields (Buttenfield and McMaster, 1991). In the present case the generalization is done by averaging 2×2 non-overlapping windows (De Cola, 1994).

Table 1 describes a power-2 grid pyramid of size $L = 10$ ($2^L = 2^{10} = 1024$) based on 31.25-m data. The columns of the table show level l, which indexes the layers of the pyramid, the number of cells in each row (= number of cells in each column), and the size of each cell. Three types of data are also shown for reference, from 1000-m advanced very high resolution radiometer (AVHRR) cells, through 30-m Landsat TM, to 1-m digital orthophoto quad imagery. In this chapter the word grid is used to refer to imagery or raster data to convey the idea that these operations could be performed on any kind of rectangular array.

Table 1 Description of Pyramids Used in this Chapter and Comparisons with Other Grid Data

Level	Cells in each row	Cell size (m)	Grid data examples	Typical regions
13	0.125	256,000		Chesapeake Bay
12	0.25	128,000		1 degree
11	0.5	64,000		
10	1	32,000		
9	2	16,000		1:24,000 USGS quad
8	4	8000		
7	8	4000		
6	16	2000		
5	32	1000	AVHRR	
4	64	500		
3	128	250		
2	256	125		
1	512	62.5		
0	1024	31.25	Landsat TM	
–1	2048	15.62		
–2	4096	7.81		
–3	8192	3.91		
–4	16384	1.95		
–5	32768	0.98	DOQ	

It should be noted that in $E = 2$-dimensional space, *Vol*, the volume of data (or number of cells, for example in bytes; see Light, 1986) of a pyramid is only 1/3 greater than that of its lowest level. This advantage is even greater for 3-dimensional pyramids, for which the additional size is only 1/7. In fact, for any physical space of E dimensions, the ratio of the size of a pyramid and that of its lowest level is

$$Vol(\{A\})/Vol(\{A_0\}) = 2^E/(2^E - 1) \quad (3)$$

and this ratio $\rightarrow 1$ as $E \rightarrow \infty$, so the savings realized by generalization become quite dramatic for high-dimensional data structures (for a practical example of data reduction by resolution manipulation see Nozette et al. (1994)).

The highest level L represents how far the generalization operation $g(\ )$ can proceed until there is one object (point location or grid cell mean) corresponding to the "scope" or maximum extent of the data (Schneider, 1994), which may also be the highest level of interest. L should also be larger than the "characteristic scale" of the phenomenon; if we are trying to understand grizzly bear habitats, for example, the physical extent of our data should span a region at least as large as that occupied by the animals during a yearly breeding cycle. But again this relates more to Quattrochi's 4th process-level problem, which this technical chapter will not address.

Multiresolution Variance

The visualization of data pyramids is quite common; indeed, all grids can in some sense be regarded as generalizations of the real-world data on which they are based, and most practical visualizations are further generalized (for display, transmission, or analysis) from some lowest-level dataset. There are also many ways to characterize such pyramids quantitatively. The mean values of the $\{A_l\}$ for each l can serve as a check on the generalization (this series should be unchanging to within a given level of tolerance). The variance $\sigma^2(A_l)$ of the pyramid levels is sensitive to spatial structure (Arbia, 1990). In the case of a random field, $\sigma^2(A_{l+1}) \approx \sigma^2(A_l)/2^E$, where E is the dimension of the physical space in which the data lie.

The scaling characteristics of the variance can be determined from

$$\sigma^2(A_l) = a(2^l)^b \tag{4}$$

where a is predicted variance at level-0 and b is an (inverse) index of spatial autocorrelation that varies between $b = 2$ for random data and $b = 0$ for extremely simple data such as a polygon (De Cola, 1994). This scheme implies that any particular dataset lies at a point in the scale dimension, and the techniques presented here allow us to explore this dimension; but only in one direction, for although we can aggregate data from level $l = 0$ to higher (coarser) levels, we cannot move in the other direction ($l < 0$) with any certainty. (Table 1, therefore, only suggests the existence of lower-level data for this study; although such data exist, they cannot be created with perfect accuracy from higher levels.) This does not deny that there is a wide range of tools, such as interpolation and kriging, for moving down the scale continuum (Cressie, 1991), but such approaches correspond to forecasting in the time dimension, which is speculation, not history.

This treatment of scale as a line segment that spans a range from the finest available resolution of the data to a single summary statistic, rather than as a single point or as a number of discrete points, highlights the pyramid as a nested set in which the variance of each resolution level consists of the variances of the levels above plus some new information (signal or noise), so that the so-called scaled variance

$$\Delta\sigma_l^2 = \sigma^2(A_l) - \sigma^2(A_{l+1}) \tag{5}$$

is of interest (Justice, Townshend, and Kalb, 1991). This approach is based on the idea of nested variation in which movement down the resolution scale (from coarse to fine) may reveal structure at some level (Moellering and Tobler, 1972). This may happen when the spatial organization of the source data lies around the middle of the random-to-simple continuum (De Cola, 1991). As the analysis increases resolution, there is the expectation that variance $0 \leq \Delta\sigma_l^2 \leq 4$. When little additional variance is found a relatively spatially coherent feature may be detected; when considerable additional variance is found there is probably noise at that level. This argument obviously requires variable resolution data rather than data from a few distinct resolutions. It should be noted that a richer resolution-based characterization of the spatial complexity is afforded by scaling various dimensions, but this treatment would require a digression into multifractality, pursued elsewhere in this book (see Chapter 16).

Composition of Aggregation with Other Operators

An important research issue is the problem of the composition of aggregation and other operations on grids. Consider for example some operator $f(\ )$ that transforms grids. It is possible to examine $f(A_l)$ as well as $g(f(A_l))$, its generalization. The question is whether

$$f(g(A_l)) = g(f(A_l))? \tag{6}$$

We need to know if these operations are commutative for at least three reasons. First, it is theoretically interesting to know if Eq. 6 holds or nearly does. Second, the scaling behavior of the operator $f(\ )$ may tell us something useful about the phenomenon (for example, that the slope of elevation data is not self-similar). Third, it may be much faster to generalize and then transform the data, producing $f(g(A_0))$, than to transform the low-level data and then generalize the result, producing $g(f(A_0))$. This will particularly be true if f is computationally intensive and therefore faster to perform on generalized data. If the difference is small for some purpose then we can store (or generate) $\{A\}$ (defined in Eq. 2) and perform various operations on it without having to perform each of them on the finest level data. Tobler (1979) discusses the composition, as well as inversion, of operations in a different context.

This is a relatively unexplored issue, and yet it is important for the management and analysis of large datasets. For example, is there an important difference between computing an index (say NDVI) from two or more level-0 (30-m) TM bands and then aggregating the results to some coarser level, vs. aggregating the bands and then computing the index? If any operator is substituted for the normalized difference vegetation index (NDVI) computation, this question becomes general and is relevant to issues of data storage and computational speed, as well as interpretation of

processes and features. And of course beyond questions of computational efficiency, it is also useful to know just how such transformations scale.

Multiresolution Covariation

When we have characterized the scaling of one set of measurements, interest turns to one or more other datasets $\{B\}$ and their comparisons with $\{A\}$. Again, the sequence of steps is as above: visualization, analysis of variation, and other operations. As with any analysis of covariation we are concerned with statistical criteria of difference. Another approach is to examine the scaled variances $\Delta\sigma_l^2$ (Equation 5) to determine if $\{B\}$ is sensitive to the same scale breaks as $\{A\}$. Finally, we can examine scatter diagrams and correlation coefficients to compare the grids. Large correlation values are necessary but not sufficient conditions for strong process linkages between A and B.

Another obvious way to compare data is to examine multiresolution covariation $Cov(A_l, B_l)$. The most general statement of this situation is the modifiable area unit problem (Fotheringham and Wong, 1991). This series tells us not only about similarities between A and B but also about the scale structure of their association (Arbia, 1990). This issue will be explored in detail below.

The multiresolution analysis of data uses a *Mathematica* package of seven major modules, each of which has several related functions (Wolfram, 1991). (NOTE: Any use of trade, product, or firm names in this chapter is for descriptive purposes only and does not imply endorsement by the U.S. Government.) Table 2 outlines the functions in the package, and is shown to highlight the basic tools that are necessary for multiresolution grid analysis. The package requires statistical and visualization functions as well as tools that provide information about data or perform normalization (Abramowitz and Stegun, 1965). Data input/output and the NDVI transformation are included next, and then basic statistical operations. Visualization is handled by programs that display data in 2-D, 3-D, or arrayed by resolution. The scale operations themselves make pyramids and either expand (replicate) or interpolate grid data. Finally, a number of multiscale tools analyze the data at multiple levels.

STUDY AREA AND DATA SOURCES

Techniques are driven both by theory and practical needs. The USGS distributes and regularly uses three major grid data series: 1-m digital orthophotoquads (DOQ), 30-m Landsat TM (Lillesand and Kiefer, 1987), and 1000-m AVHRR, whose resolutions are compared in Table 1. An important challenge in the management and use of these data is the characterization of the land not only at multiple resolutions (in this case 3) but at a continuous range of resolutions spanning three orders of magnitude or 10 powers of 2.

The USGS is currently conducting research that uses vector and raster data to develop new ways of mapping the land in space and time (Kirtland et al., 1994). A current research project, for example, focuses on human-induced land transforma-

Table 2 The *Mathematica* PYRAMID System

(* INITIALIZATION *)
Needs["Statistics`DescriptiveStatistics`"]
Needs["Graphics`Graphics`"]
Needs["Statistics`LinearRegression`"]
Install["/home/nmd/ldecola/math/binary"]
(* A FEW BASIC TOOLS *)
showmem.m
vartable.m
ndvi.m
(* DATA INPUT & OUTPUT *)
readdata.m
writepyr.m
window.m
(* STATISTICS *)
range.m
normalize.m
var.m
invnorm.m
standardize.m
report.m
plotcdf.m
(* VISUALIZATION *)
plotdensity.m
pyrarray.m
drape.m
(* AGGREGATION, REPLICATION, INTERPOLATION *)
makepyr.m
expand.m
interp.m
(* PYRAMID ANALYSIS *)
multvar.m
msscatter.m
corr.m
mscorr.m

tions both in central California and in the upper Chesapeake Bay. Urbanization in the latter region focuses on the Baltimore/Washington metropolis (Acevedo, Foresman, and Buchanan, 1996), which is shown in Plate 1* as a perspective rendering with AVHRR NDVI data draped on digital elevation data for level 9 (16-km) and level 5 (1-km). This figure illustrates one of the uses of multiresolution techniques. The example on the top is based on mapping the NDVI values on a brown-to-green hue spectrum and required less than 1 second of processing time on an IBM RISC/6000 model 590 with 128 MB of memory running at approximately 93 Mflops. The view on the bottom required 3 minutes.

We are interested not only in the synoptic characteristics of a region, but also in gaining more detailed information about the Baltimore area and specifically four

* Color plates follow numbered page 168.

cells from the level-9 data shown in the top frame of Plate 1. Plate 2* shows the location of the data for both the 256^2-pixel AVHRR grid and the 1024^2-pixel TM grid. The figure illustrates how the AVHRR dataset gives a synoptic view of the region and the TM data provides more detailed information about the city of Baltimore. This visualization also suggests the way that data sources span the scale space mentioned above. The fact that these two sensors span a resolution range of over five levels ($\text{Log}_2(1000/30) = 5.06$) makes comparisons between them difficult.

Table 3 outlines the steps that were taken to conflate the two datasets. The AVHRR Baltimore scene was extracted from a 1990 CD-ROM that contained biweekly data for the U.S. at 1000-m resolution. This established the base projection and level-5 resolution standard for the study. The other dataset is a Landsat TM grid that was created as follows. A 2048^2-pixel 7-band, 30-m grid was first georectified using 1:100,000 scale USGS maps, resampled to 31.25 m, and then reprojected to Lambert Equal Area. A 1024^2-pixel window was extracted, resulting in an error of no more than 100 m between the two grids. Note that square power-2 grids are used throughout to facilitate aggregation.

Table 3 Steps in Conflating the Two Datasets

	Landsat TM →		AVHRR ←	
Date	1998/07/06		1990/06/22–07/05	
Data	7 bands	NDVI	NDVI	7 bands
Location	Chesapeake	Baltimore	Baltimore	U.S.
Coverage	32,000 km²	1,024 km²	1,024 km²	13 M km²
Projection	SOM[a]	Lambert	Lambert	Lambert
Resolution	30 m	31.25 m	1000 m	1000 m
Level	–0.133[b]	0	5	5
Data volume	40 MB	1024^2 bytes	32^2 bytes	13 MB

[a] Space Oblique Mercator.
[b] Shown for reference only; level is typically an integer.

There are obvious difficulties with the conflation used here (as opposed to the use of two sensors with identical spectral response imaging the same region at the same time). At the finest spatial resolution near level-0 the data are subjected to varying degrees of modification in the process of resampling and reprojecting. Temporally, the data were collected at different points in time. And spectrally, the sensors have different wavelength sensitivities. It is therefore difficult to determine exactly what the effects of these inherent and pre-processing differences are; yet, as we shall see, these differences significantly diminish at coarser resolutions.

ANALYSIS

The two color plates illustrate that the simplest yet often most powerful form of analysis is the visualization of data directly at multiple resolutions and from multiple

* Color plates follow numbered page 168.

sources (Valenzuela and Baumgardner, 1990). Layers from a Landsat NDVI pyramid for the Baltimore region are shown in Figure 1. For example, each of the odd-valued levels reveals something new about the region:

- The coarsest level-9 (16-km, the resolution of the top picture in Plate 1) reveals the bifurcation of the region into three high/medium NDVI cells and one low NDVI cell.
- Level-7 shows the northwest trend of the data, indicating that the urban area is a region of depressed vegetation values.
- Level-5 locates such general features as the city of Baltimore and Loch Raven to the north of the city.
- Level-3 shows the outline of the lake, the Inner Harbor, and the road network.
- Level-1 does not reveal much more detail at the resolution of this printed grid (another advantage of pyramids is that they allow the use of appropriate resolution in visualization).

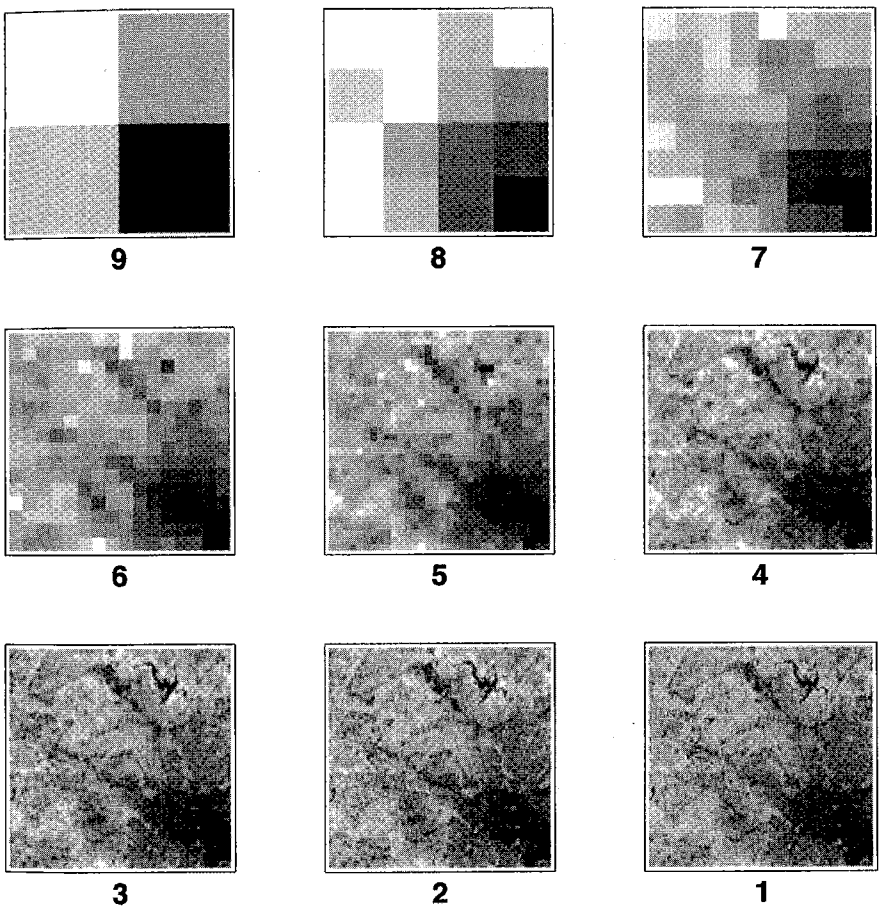

Figure 1 Nine levels from the Baltimore Landsat TM NDVI grid pyramid, from 16,000-m to 62.5-m resolution.

Multiresolution Analysis of Landsat Data

Beyond visualization, data pyramids are also useful in multiresolution data exploration. Because it seems that the size and complexity of our data will always surpass the capacity and speed of our computers, the grid pyramid provides a data structure that can be used for rapid analysis of higher-level data in preparation for lower-level processing.

Statistical description is extremely useful in understanding data; indeed, it is a way of exploring data at coarser scales. Figure 2 is a plot of the cumulative frequencies of the TM NDVI data (SAS Institute, 1990) and shows that negative skewness is apparent even at low resolution. Although the central limit theorem predicts that higher pyramid levels will become increasingly normal, this is only necessarily true if the data are not autocorrelated, which is not the case for geographic information (Griffith and Amrhein, 1990). The higher-level plot is quite adequate to detect this pattern and involves the analysis of 1/16 as much data.

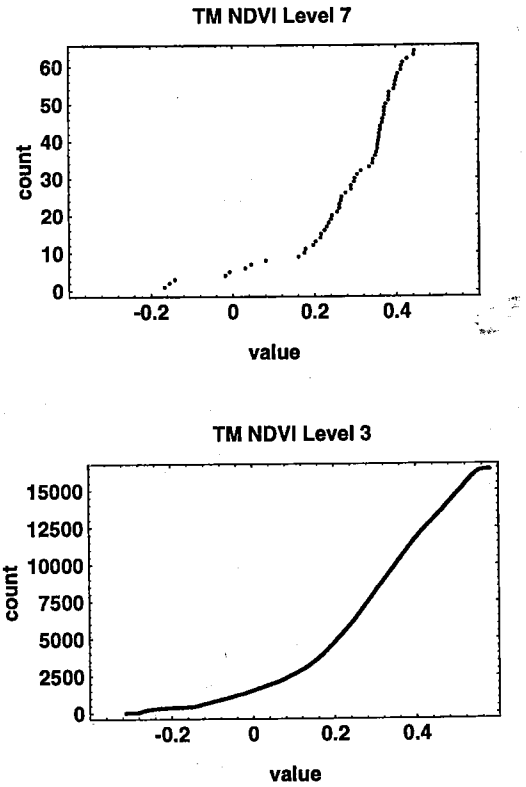

Figure 2 Cumulative frequency plot of the Baltimore TM NDVI grid at level-7 and level-3.

Table 4 reports these and other statistics for three levels of the TM NDVI pyramid. The first row shows l, the level of the pyramid, and the next row gives N,

Table 4 Statistics for Three Levels of the TM NDVI Pyramid

Level	7	5	3
N	64	1024	16384
Min	−0.167373	−0.29294	−0.311943
Max	0.444665	0.545052	0.58007
Mean	0.276787	0.276787	0.276787
HarmonicMean	1.04045	0.341917	0.175422
Median	0.324276	0.30883	0.300726
Variance	0.0208468	0.0265988	0.0339747
StandardDeviation	0.144384	0.163091	0.184322
SampleRange	0.612038	0.837992	0.892013
MeanDeviation	0.107143	0.125597	0.145518
MedianDeviation	0.0659448	0.0943039	0.118861
QuartileDeviation	0.0719152	0.0978015	0.119147
Skewness	−1.49307	−1.12243	−0.7984
QuartileSkewness	−0.344965	−0.124794	−0.0319378
KurtosisExcess	1.77709	1.12823	0.331785

the number of rows (= number of columns = $(2^{(L-l)})^2$). The next two rows report the extrema of these levels, and as expected this range increases at finer resolutions. The mean of the levels is constant, as it should be with aggregation by averaging (such other aggregation techniques as resampling, nearest neighbor selection, cubic convolution, might not have this property). The median, however, declines as negative skewness lessens. Variance and the other measures of variation increase at lower (finer) levels, as we expect for all but the most coherent data. The only statistic that behaves counterintuitively is skewness, which would be expected to increase at lower levels, as does the variance.

Another way to examine multiresolution variation is to consider the differences between variances at each resolution level. Figure 3 shows how much variance is added at each successive resolution level (Equation 5) and therefore is best interpreted from right to left. For all empirical data this addition is $\Delta\sigma_l^2 \geq 0$, and the plot suggests for this study area a scale break at level-6, i.e., the existence of coherent structure at around 2000 m (see Table 1 above). This is interesting because it is close to the resolution of the AVHRR data analyzed below. One theory is that the patch size at which urbanization — and particularly the transportation network — interacts with vegetation may be roughly a kilometer.

A question asked above in Equation 6 was whether $f(g(A)) = g(f(A))$? Does an operation performed on aggregated data give the same result as the aggregation of data on which the operation is first performed? To explore this issue, consider the vegetation index

$$\text{NDVI} = (\text{NIR} - \text{RED})/(\text{NIR} + \text{RED}) \tag{7}$$

which is obviously nonlinear (Hall, 1992). NDVI was first computed using level-0 TM RED and near infrared (NIR) data and then the NDVI pyramid was created and denoted PYR(NDVI) to reflect the priority of the vegetation transformation. Pyramids were also created from each of the NIR and RED grids and then NDVI was

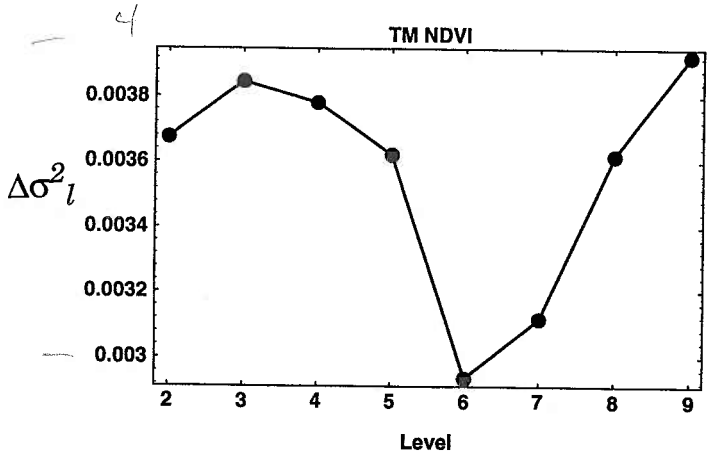

Figure 3 Multiscale variation differences for the TM NDVI data; read from right to left, the variance added at each finer resolution scale is shown.

computed for each of the levels, resulting in a data structure called NDVI(PYR) because the pyramids were created first.

In general, the results are close but not identical, as shown in Figure 4, which is a level-7 (4000-m) scatter diagram. The figure implies that, although there is some difference between the operations, they appear to be generally commutative. It is curious that the exception seems to be one particular 16-km^2 grid cell for which the difference is about 10%. It is not known whether this type of anomaly (in which a few cells do not conform to the rule) would be present for other types of data or regions; this is clearly a topic for further investigation. Yet overall the results are virtually identical (r = 0.995). Although we cannot assume the strict commutativity of aggregation and NDVI, for many purposes the results are likely to be acceptable (but there may well be transformations more complex than NDVI for which commutativity will not hold).

This exploration of commutativity between the NDVI and the pyramid operation was not carried out for other grids, as the focus here is on the development of tools and ideas for two datasets readily at hand. Much further work needs to be done to determine if this close correspondence is true across time, over space, and for other kinds of data and transformations. Positive results would allow data providers to supply users with aggregated versions of raw data and let them compute their own indices rather than supply the indices themselves. This finding has interesting implications for the management of a national spatial data infrastructure (NSDI). If, for example, there is not much difference between NDVI computed from aggregated RED and NIR data vs. aggregated NDVI data, then a data clearinghouse might just as well archive the raw highest-resolution data and supply it to a user needing a specific resolution of data (or, indeed, some other transformation).

In the present case, for example, users would like to know if the result of downloading 32-km NDVI data would be nearly the same if they acquired two 1-km datasets — about 2000 times the data volume — and performed the NDVI operation locally. Putting these issues aside, we assume at least in the present case

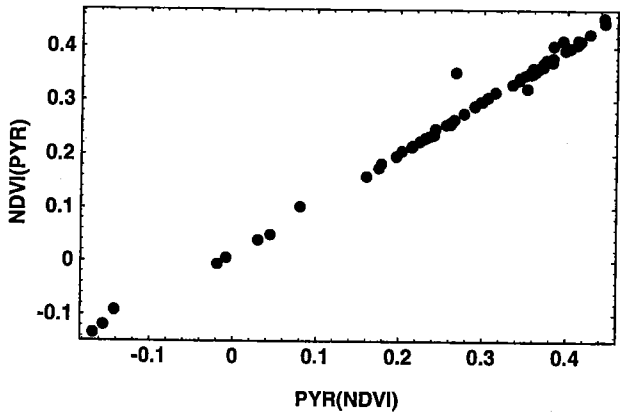

Figure 4 Scatter diagram comparing the result of NDVI computed from level-6 of a RED and a NIR pyramid with level-6 of a pyramid aggregated from a level-0 NDVI grid.

that aggregation and transformation are commutative and base the analysis to follow on PYR(NDVI), in which a pyramid was based on a 0-level NDVI grid.

Cross-Sensor Covariation

Many of the chapters in this book show that the need to integrate data among widely disparate sources drives much of the research into scaling in spatial data. For example, the USGS uses TM and AVHRR data to develop new land characterization products (Loveland et al., 1991). The tools developed here can be used to compare data not only from the various resolutions and grids (bands) of a given data source, but also from two distinct datasets. Table 3 showed how windowing, NDVI computation, reprojection, resampling, and finally aggregation were used to create a multiresolution representation of the Baltimore region. Figure 5 compares the level-5 TM NDVI and the level-5 AVHRR NDVI. Visual inspection of the TM and AVHRR NDVI data suggests that the correspondence is close: both show the city and the low-vegetation radial corridors, although the TM grid, based on 32×32 pixel averaging of high-resolution data, appears to be slightly sharper.

The scatter diagrams in Figure 6 illustrate this cross-sensor covariation at three resolutions, from level-9 (16,000-m), through level-7 (4000-m), down to level 5 (1000-m). (The difference in units is due to the fact that the TM NDVI data were not normalized to a 0...255 range.) The top graph shows that TM and AVHRR both detect two regions of high and low values (see the first frame of Figure 1). But the finer-resolution diagrams reveal considerable variation between the datasets. The correlation (Table 5) is nearly linear at level-9, where there are only four $(16\text{-km})^2$ cells, one of which is a single low-greenness cell corresponding to Baltimore and its harbor. The association is still quite strong at level-7, but declines to $r = 0.82$ for the 1024 cells at level-5. This is also the largest drop in correlation, just as the largest increase in variance was from level-6 to level-5. If we are interested in comparing the two sensors, the coarser-resolution correlations will, as with any autocorrelated

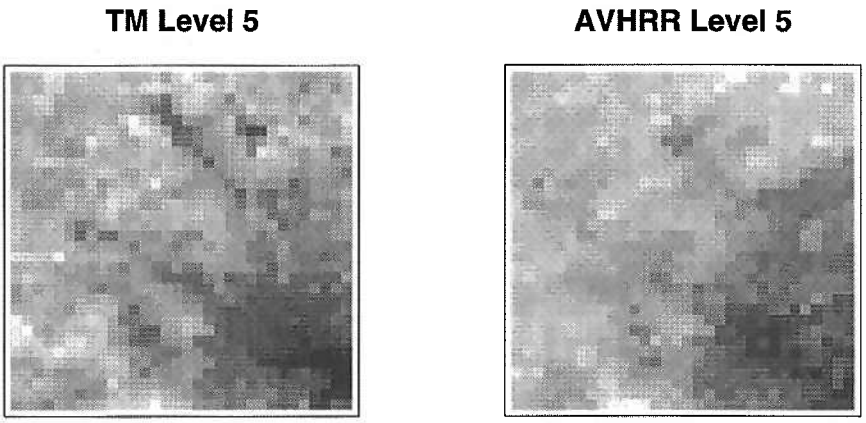

Figure 5 Comparison of TM and AVHRR NDVI data at level-5 (1000 m).

data, overestimate the association. Scaling illustrates the degree of autocorrelation: generalization has a weaker effect on spatially autocorrelated than on non-autocorrelated data. This confirms everyday experience that structure is scale-dependent; if a strong pattern exists it will be visible at multiple levels, and any pattern — save that of a true fractal set — will eventually break up at finer resolutions.

A particularly striking way to view the differences in these grids is by visualizing the differences between two pyramids: $\{A\} - \{B\}$ (see Equation 2). Figure 7 shows the differences between the AVHRR and TM NDVI values. The left side of Figure 7 shows $AVHRR_5 - TM_5$: the differences between the NDVI values at level-5. The right side shows $(AVHRR_6 - TM_6)$, the level-6 differences linearly interpolated to level-3 (250-m) and then contoured. The interpolated image on the right shows a radial pattern in which the AVHRR NDVI values are generally higher than those of the TM data along major transportation routes (recall that level-6 was shown in Figure 3 to be the level at which scaled variation is at a minimum). This difference may be due to temporal change (2 years separate the grids) as well as to the possibility that the resolution of the AVHRR sensor differs from the effective resolution of the generalized TM data. But these results should not obscure the strong correlation (Table 5) between these two datasets. This exhibit also shows the use of three different resolution levels: level 5, at which the two grids are compared; level 6, used as the basis for a fine scale contour at level 3, which makes the underlying contoured pattern easier to see.

The point of this comparison is not that the two sensors are similar, because whatever differences that exist are only significant in a particular context. For some purposes AVHRR data simply will not provide the accuracy of TM data, while for others the latter may burden analysis with needless spatial detail, too much data, and excessive processing time. A purely technical approach (exploring such issues as corrections, calibrations, sampling, and interpolation) would be necessary to determine either to what extent, for example, aggregated TM NDVI data might be substituted for AVHRR data, or indeed whether interpolated AVHRR data might adequately replicate TM data. The visual, scatter diagram, and correlation compar-

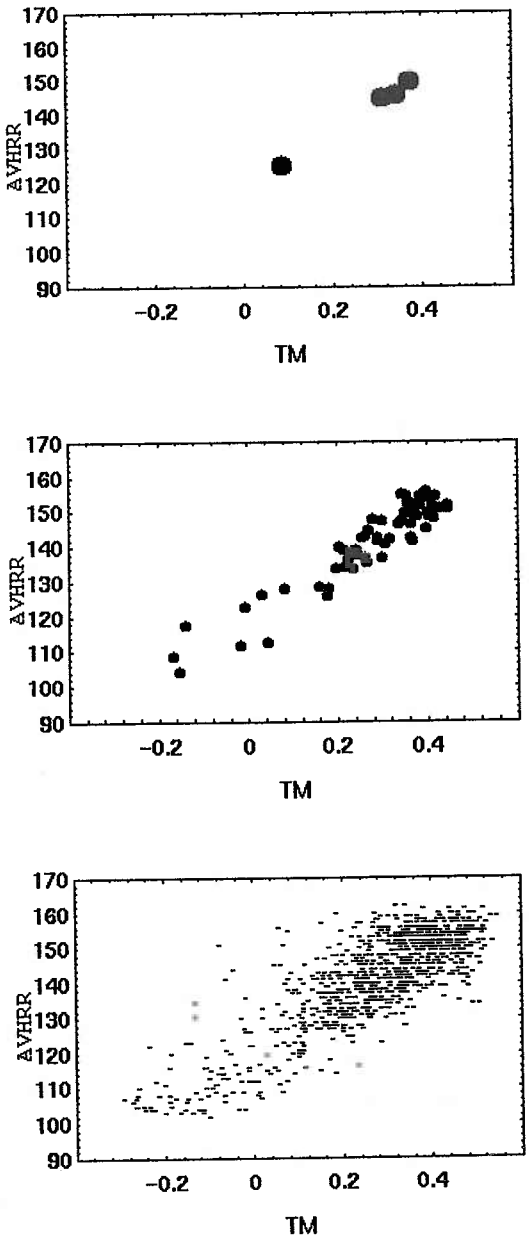

Figure 6 Scatter diagrams of AVHRR vs. TM NDVI at levels 9, 7, and 5. Only the AVHRR values were scaled to 0 to 255 range.

isons illustrate rather that each sensor provides an observation within the dimensions of space/time/feature/scale and that these observations can be compared and even substituted for one another in the appropriate circumstances.

Table 5 Correlations Between TM and AVHRR NDVI Data

Level	Correlation
9	0.997
8	0.966
7	0.942
6	0.883
5	0.819

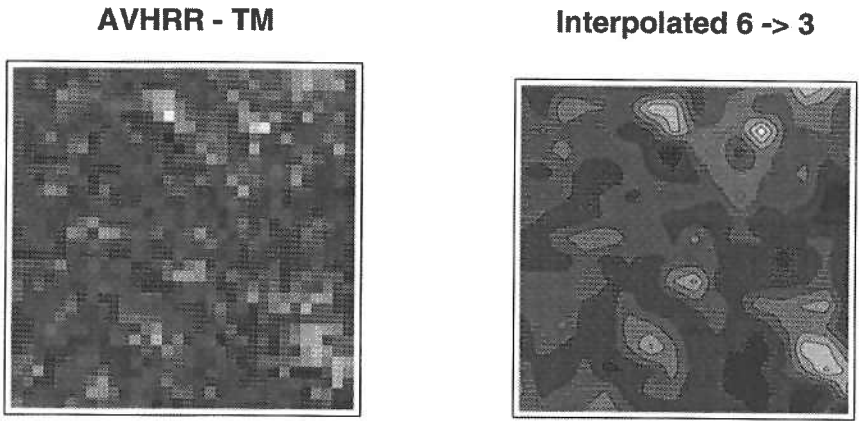

Figure 7 Difference between standardized AVHRR and standardized TM grids. At left is the level-5 (1000-m) difference grid; at right is the result of taking a level-6 (2000-m) difference grid, linearly interpolating to level-3 (250-m), and then contouring.

CONCLUSION

This chapter illustrates the creation, visualization, and statistical analysis of multiresolution grid pyramids. Such pyramids are only 1/3 larger than the 0-level data on which they are based (and these advantages improve with the dimensionality of the data), and they give a richer view of patterns and phenomena. The multiresolution approach allows the rapid prototyping of functions, transformations, and analytical tools; operations at any level $l + k$ are typically up to 4^k times faster than at level l; and, given the near self-similarity of data, the results are often excellent approximations of finer analysis. Multiresolution techniques also provide useful variance and covariance scaling statistics that can detect spatial structure.

These techniques were used to explore alternative measures of NDVI. For TM NDVI we find that aggregation is nearly commutative with the NDVI transformation, suggesting that there may be less need to supply users with transformed data based on lower levels than with algorithms for such transformations. Although a strong correlation between the Landsat TM and AVHRR NDVI measures was evident, there are regions of positive and negative differences, probably due, in declining order, to:

1. Temporal change
2. Inherent disparities between the two sensors
3. Differences in calibration, correction, etc.
4. Misregistration

As with all spatially autocorrelated data, the correlations decrease at finer resolutions. Nevertheless, TM data aggregated to 1 km may do a better job of detecting features than does AVHRR, particularly as this spatial level may be near the significant physical scale level at which transportation/urbanization and vegetation interaction take place.

This work provides insights into the effects of resolution changes (generalization and interpolation) of data. Whereas such transformations are usually performed in order to alter the visual appearance of an image (or map), they may also have important effects on the statistical behavior of the data. This analysis is based on the notion that scale is a bounded continuum. Although aggregation creates a pyramid from the bottom up, data exploration is more fruitful if pursued top down or "forward" from coarse to fine, just as it is more logical to follow history from the past to the present. (This insight provides one reason why astronomy has been such a fruitful science; information had to be painstakingly wrung out of coarser resolution levels before improved instruments provided more data.)

In a spirit of exploration, this book calls for greater freedom to analyze and visualize data along the scale continuum. The development of remote sensors spanning a wide range of spatial, spectral, and temporal resolutions provides scientists with precise samples along those continua. Spatial analysis, informed by a scale-sensitive insight into complexity (Steinbeck, 1977), represents a maturing of this evolution, enabling scientists to explore the minutely small and the vastly large, accepting no one scale as truth, and calling for multiple representations of the geographic world.

REFERENCES

Abramowitz, M. and Stegun, I. A., *Handbook of Mathematical Functions,* Dover, New York, 1965.

Acevedo, W., Foresman, T. W., and Buchanan, J. T., Origins and philosophy of building a temporal database to examine human transformation processes, in *ASPRS/ACSM Annual Meeting Technical Papers,* 1, 148, 1996.

Arbia, G., *Spatial Data Configuration in Statistical Analysis of Regional Economic and Related Problems,* Kluwer Academic Publishers, Boston, 1990.

Basseville, M., Beneviste, A., Chou, E. C., Golden, S. A., Nikoukhah, R., and Willsky, A. S., Modeling and estimation of multiresolution stochastic processes, *IEEE Trans. Infor. Theory,* 38(2), 766, 1992.

Bian, L. and Walsh, S. J., Scale dependencies of vegetation and topography in a mountainous environment of Montana, *Prof. Geogr.,* 45(1), 1, 1993.

Buttenfield, B. P., Object-oriented map generalization: modeling and cartographic considerations, in *Eur. Sci. Found. Meet. Generalization, Compiegne, France*, 1994.

Buttenfield, B. P. and McMaster, R. B., *Map Generalization: Making Rules for Knowledge Representation,* Longman, New York, 1991.

Cressie, N. A. C., *Statistics for Spatial Data,* John Wiley & Sons, New York, 1991.

Cullinan, V. I. and Thomas, J. M., A comparison of quantitative methods for examining landscape pattern and scale, *Landscape Ecol.,* 7(2), 211, 1992.

De Cola, L., Fractal analysis of multiscale spatial autocorrelation among point data, *Environ. Plan. A,* 23, 545, 1991.

De Cola, L., Simulating and mapping spatial complexity using multiscale techniques, *Int. J. Geogr. Infor. Sys.,* 8(5), 411, 1994.

Fotheringham, A. S. and Wong, D. W. S., The modifiable areal unit problem in multivariate statistical analysis, *Environ. Plan. A,* 23, 1024, 1991.

Frank, T. D., Tweddale, S. A., and Knapp, D. D., Variability of at-satellite surface reflectance from Landsat TM and NOAA AVHRR in Death Valley National Monument. *Photogr. Eng. Remote Sensing,* 60(10), 1259, 1994.

Franklin, S. E., Discrimination of subalpine forest species and canopy density using digital CASI, SPOT PLA, and Landsat TM data, *Photogr. Eng. Remote Sensing,* 60(10), 1233, 1994.

Getis, A. and Franklin, J., Second-order neighborhood analysis of mapped point patterns, *Ecology,* 69, 473, 1987.

Griffith, D. A. and Amrhein, C. G., *Statistical Analysis for Geographers,* Prentice-Hall, Englewood Cliffs, NJ, 1990.

Hall, F. G., Satellite remote sensing of surface energy balance: success, failure, and unresolved issues in FIFE, *J. Geophys. Res.,* 97, (D17) 19061, 1992.

Jensen, J. R., *Introductory Digital Image Processing,* Prentice-Hall, Englewood Cliffs, NJ, 1986.

Justice, C. O., Townshend, R. G., and Kalb, V. L., Representation of vegetation by continental datasets derived from NOAA-AVHRR data, *Int. J. Remote Sensing,* 12(5), 991, 1991.

Kirtland, D., De Cola, L., Gaydos, L., Acevedo, W., Clarke, K., and Bell, A. C., Analysis of human-induced land transformations in the San Francisco Bay and Sacramento Area, *World Resour. Rev.,* 6(2), 206, 1994.

Lambin, E. F., Walkey, J. A., and Petit-Maire, N., Detection of holocene lakes in the Sahara using satellite remote sensing, *Photogr. Eng. Remote Sensing,* 61(6), 731, 1995.

Light, D. L., Mass storage estimates for the digital mapping era, *Photogr. Eng. Remote Sensing,* 52(3), 419, 1986.

Lillesand, T. M. and Kiefer, R. W., *Remote Sensing and Image Processing,* John Wiley & Sons, New York, 1987.

Loveland, T. R., Merchant, J. W., Ohlen, D. O., and Brown, J. F., Development of a land cover characteristics data base for the conterminous U.S., *Photogr. Eng. Remote Sensing,* 57(11), 1453, 1991.

Meentemeyer, V. and Box, E. O., Scale effects in landscape studies, in *Landscape Heterogeneity and Disturbance,* M. G. Turner, Ed., Springer-Verlag, New York, 1987, 15.

Moellering, H. and Tobler, W. R., Geographical variances, *Geogr. Anal.,* 4, 34, 1972.

Nozette, S., The Clementine mission to the moon: scientific overview, *Science,* 266(5192), 1835, 1994.

Peuquet, D., It's about time, *Ann. Assoc. Am. Geogr.,* 84(3), 1993.

Quattrochi, D. A., The need for a lexicon of scale terms in integrating remote sensing data with geographic information systems, *J. Geogr.,* 93(5), 206, 1993.

Richards, J. A., *Remote Sensing Digital Image Analysis: An Introduction,* Springer-Verlag, New York, 1986.

Samet, H., *Applications of Spatial Data Structures,* Addison-Wesley, Reading, MA, 1989.

SAS Institute, *SAS Procedures Guide, Version 6,* 3rd ed., SAS Institute, Cary, NC, 1990.

Schneider, D. C., *Quantitative Ecology: Spatial and Temporal Scaling,* Academic Press, San Diego, 1994.

Steinbeck, J., *The Log from the Sea of Cortez,* Penguin, New York, 1977.

Stoms, D. M., Scale dependence of species richness maps, *Prof. Geogr.,* 46(3), 346, 1994.

Tobler, W. R., Smooth pycnophylactic interpolation for geographical regions, *J. Am. Stat. Assoc.,* 74(367), 519, 1979.

Turner, M. G. and Gardner, R. H., Eds., *Quantitative Methods in Landscape Ecol.,* Springer-Verlag, New York, 1992.

Valenzuela, C. R. and Baumgardner, M. F., Selection of appropriate cell sizes for thematic maps, *ITC J.,* 1990(3), 219, 1990.

Wolfram, S., *Mathematica: A System for Doing Mathematics by Computer,* Addison-Wesley, Reading, MA, 1991.